

Structural behavior of the suspen-dome structures and the cable dome structures with sliding cable joints

Hongbo Liu¹ and Zhihua Chen^{*1,2}

¹*Department of Civil Engineering, Tianjin University, Tianjin 300072, China*

²*Tianjin Key Laboratory of Civil Engineering Structures and New Materials, Tianjin 300072, China*

(Received January 9, 2012, Revised May 7, 2012, Accepted May 17, 2012)

Abstract. Sliding cable joints have been developed for the cable dome structures and the suspen-dome structures to reduce the cable pre-stressing loss and obtain a uniform inner force in each hoop cable. However, the relevant investigation is less addressed on the structural behavior of the cable dome structures and the suspen-dome structures with sliding cable joints due to the lack of analysis techniques. In this paper, a closed sliding polygonal cable element was established to analyze the structural behavior of the cable dome structures and the suspen-dome structures with sliding cable joints. The structural behaviors with sliding cable joints were obtained.

Keywords: cable dome structures; suspen-dome structures; sliding cable joint; closed sliding polygonal cable element; structural behavior

1. Introduction

Cable dome structures were developed by Geiger and the structures were adopted in the gymnasiums and the stadiums for the Summer Olympics at Seoul, Korea in 1986 (Geiger 1986). As an innovative and lightweight dome system, cable dome attracts a lot of attention from engineers. The cable domes have been widely used in large span structures, such as the Redbird Arena and the Sun Coast Dome. The largest existing cable dome—Georgia Dome—with an elliptical plan, was designed for the Atlanta Olympic Games in 1996. Further, the construction, design, and structural behaviors of cable domes have been extensively studied (Kawaguchi 1999, Yuan 2002, 2003, 2007, Kim 2003). Similarly, suspen-dome structures were proposed by Kawaguchi (1999). It has been widely applied in the gymnasium roofs, such as Hikarigaoka Dome and Fureai Dome in Japan, Tianjin Baoshui Commercial Exchange Center in China, Badminton Gymnasium for 2008 Beijing Olympic Games in China, Jinan Olympic Sports Center's Gymnasium for the 2009 11th National Olympic Games in China, etc. Many investigations have been performed on the suspen-dome structures through experimental research and numerical analysis. The structural mechanism of typical suspen-dome has been well understood by researchers and engineers (Kang 2003, Cui 2004, Kitipornchai 2005, Chen 2005, Zhang 2007, Wang 2007, Zhang 2008, Cao 2010).

With the development of suspen-dome structures and cable dome structures in practical

*Corresponding author, Ph.D., E-mail: zhchen@tju.edu.cn

engineering, some innovations have been conducted to improve their construction process and structural behavior, e.g., sliding cable joints for bottom end of strut (Chen 2010). However, a few researches have been reported on the structural behavior of the cable dome structures and the suspen-dome structures with sliding cable joints. Only Cui and Chen studied the static behavior of suspen-dome structures with sliding cable joints. In the published papers, the effect of various structural parameters on the structural behavior of suspen-dome and cable dome structures with sliding cable joints was not included.

In this paper, a closed sliding polygonal cable element was firstly presented for the structural analysis of suspen-dome structures and dome structures with sliding cable joints. And then the effect of the rise-span ratio and bearing type on the stability of suspen-dome structures and the static behavior of cable dome structures were studied using the presented cable element.

2. Formulation of the closed sliding polygonal cable element

In the current finite element analysis of the suspen-dome structures and cable dome structures, the cables have been simplified as 2-node straight bar elements separated by adjacent joints, only subjected to tension forces. However, if the sliding cable joints are used in suspen-dome structures and cable dome structures, this treatment results in the constant tension forces in all cable segments. In this situation significant error may be made with cable sliding neglected. Therefore, some techniques have been developed to consider the cable sliding based on finite element analysis with simplified separate cable elements (Cui 2004, Chen 2011). These techniques all need manual iteration intervener by engineers, which is a time-consuming job, especially for large-scale cable-strut structures. Comparatively, formulating sliding cable elements is a more convenient way to simulate sliding cables. Three-node sliding cable elements (Zhou 2004) have been developed and verified for the analysis of parachute systems and simple cable structures. But because there are many nodes in a continuous cable, this element is not suitable for the structural analysis of suspen-dome structures and cable dome structures. An opening multi-node sliding cable element (Chen 2010) was developed and applied to study the structural behavior of suspen-dome structures, but in this study, the mass matrix and body force matrix is not considered; furthermore, the continuous cable is closed in practice. Therefore, a closed continuous sliding cable element has to be formulated for cables in suspen-dome structures and cable dome structures.

Fig. 1 shows a form of closed n -node sliding polygonal cable element. In Fig. 1, the cable between the adjacent two nodes is straight. All nodes can slide along the cable to get the equilibrium position under the external forces. $S_i (i = 1, 2, \dots, n)$ in Fig. 1 denotes i th node in the closed sliding polygonal cable element. $E_i (i = 1, 2, \dots, n)$ denotes i th ($i = 1, 2, \dots, n$) cable segment in the closed sliding polygonal cable element. The internal force vector and stiffness matrix were deduced with the principle of virtual work and total Lagrange formulation. In the development of the closed sliding polygonal cable element, the following assumptions were used:

- 1) The strain is uniform along the entire element. This assumption implies that there is no resistance, such as friction, at the sliding cable joints.
- 2) The cable is ideally flexible and its bending stiffness is ignored.
- 3) The cable material variation is described with finite strain.
- 4) The constitutive relation between conjugate stress and strain is linear.

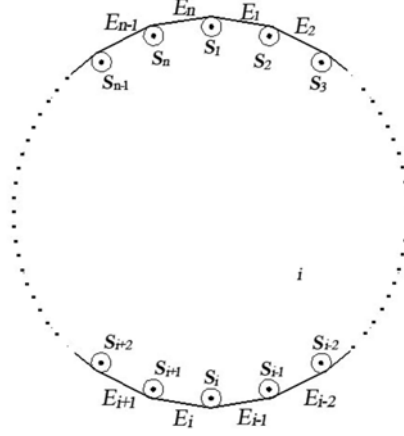


Fig. 1 Closed sliding polygonal cable element

2.1 Element internal force and stiffness

According to the above assumption, the principle of virtual work and total Lagrange formulation, the incremental virtual work done by the internal force is

$$\delta W_I = \int_L s_{11} \delta e_{11} A_0 dL \quad (1)$$

in which L stands for the initial total length of the closed sliding polygonal cable element and L is determined by initial coordinate vector $X_i, Y_i, Z_i (i = 1, 2, \dots, n)$; e_{11} stands for Green-Lagrange Strain; s_{11} stands for the second category of Piola-Kirchhoff stress (PK2 Stress); A_0 stands for the initial cross-sectional area which is invariable along the entire element. In the total Lagrange formulation, the integration is performed over the initial configuration. Because the strain and stress are assumed to be constant along the element, the integration in Eq. (1) is analytically performed.

$$\delta W_I = s_{11} \delta e_{11} A_0 L \quad (2)$$

For the closed sliding polygonal cable element, the Green-Lagrange strain is given by

$$e_{11} = \frac{l^2 - L^2}{2L^2} \quad (3)$$

in which l stands for the current total length which is determined by the current coordinate vector $x_i, y_i, z_i (i = 1, 2, \dots, n)$ of nodes according to the current geometric configuration.

The current element length l is determined by the current nodal coordinates (x_i, y_i, z_i) as

$$\begin{aligned} l &= \sum_{i=1}^{i=n} l_i = \sum_{i=1}^{i=n-1} \sqrt{(x_{i+1} - x_i)^2 + (y_{i+1} - y_i)^2 + (z_{i+1} - z_i)^2} + \sqrt{(x_1 - x_n)^2 + (y_1 - y_n)^2 + (z_1 - z_n)^2} \\ &= \sum_{i=1}^{i=n} \sqrt{(\Delta x_i)^2 + (\Delta y_i)^2 + (\Delta z_i)^2} \\ &= \sum_{i=1}^{i=n} \sqrt{(\Delta_{3(i-1)+1})^2 + (\Delta_{3(i-1)+2})^2 + (\Delta_{3(i-1)+3})^2} \end{aligned} \quad (4)$$

in which

$$\left. \begin{aligned} \Delta_{3(i-1)+1} &= \Delta x_i = x_{i+1} - x_i \\ \Delta_{3(i-1)+2} &= \Delta y_i = y_{i+1} - y_i \\ \Delta_{3(i-1)+3} &= \Delta z_i = z_{i+1} - z_i \end{aligned} \right\} (i = 1, 2, \dots, n-1) \quad (5)$$

$$\left. \begin{aligned} \Delta_{3(n-1)+1} &= \Delta x_n = x_1 - x_n \\ \Delta_{3(n-1)+2} &= \Delta y_n = y_1 - y_n \\ \Delta_{3(n-1)+3} &= \Delta z_n = z_1 - z_n \end{aligned} \right\} \quad (6)$$

The current nodal coordinates (x_i, y_i, z_i) ($i = 1, 2, \dots, n$) are related to the initial coordinates (X_i, Y_i, Z_i) ($i = 1, 2, \dots, n$) and current nodal displacements (u_i, v_i, w_i) by

$$\left. \begin{aligned} x_i &= X_i + u_i \\ y_i &= Y_i + v_i \\ z_i &= Z_i + w_i \end{aligned} \right\} \quad (7)$$

Assume that the constitutive relation between conjugate stress and strain is linear; the PK2 stress is given by

$$s_{11} = s_0 + Ee_{11} \quad (8)$$

where E stands for elastic modulus; s_0 stands for the initial stress in the cable element. The nodal displacement vector can be given by

$$\begin{aligned} \mathbf{d} &= \{u_1, v_1, w_1, u_2, v_2, w_2, \dots, u_i, v_i, w_i, \dots, u_n, v_n, w_n\} \\ &= \{d_1, d_2, d_3, d_4, d_5, d_6, \dots, d_{3(i-1)+1}, d_{3(i-1)+2}, d_{3(i-1)+3}, \dots, d_{3(n-1)+1}, d_{3(n-1)+2}, d_{3(n-1)+3}\} \\ &\quad (i = 1, 2, \dots, n) \end{aligned} \quad (9)$$

in which

$$\left. \begin{aligned} d_{3(i-1)+1} &= u_i \\ d_{3(i-1)+2} &= v_i \\ d_{3(i-1)+3} &= w_i \end{aligned} \right\} \quad (10)$$

Calculate the variation of Eq. (8) and consider the tension-only feature of the sliding polygonal cable element, we get

$$\begin{cases} \mathbf{B} = \frac{\delta e_{11}}{\delta \mathbf{d}} & s_{11} \geq 0 \\ \mathbf{B} = 0 & s_{11} < 0 \end{cases} \quad (11)$$

And

$$\{\mathbf{B}\}_{3(i-1)+k} = \frac{\delta e_{11}}{\delta d_{3(i-1)+k}} = \begin{cases} \frac{l}{L^2} \left(-\frac{\Delta_k}{l_1} + \frac{\Delta_{3(n-1)+k}}{l_n} \right) & (i = 1; k = 1, 2, 3) \\ \frac{l}{L^2} \left(\frac{\Delta_{3(i-2)+k}}{l_{i-1}} - \frac{\Delta_{3(i-1)+k}}{l_i} \right) & (i = 2, \dots, n; k = 1, 2, 3) \end{cases} \quad (12)$$

The incremental virtual work given by Eq. (2) can be rewritten as

$$\delta W_I = A_0 L s_{11} \mathbf{B} \delta \mathbf{d} = \mathbf{p} \delta \mathbf{d} \quad (13)$$

And the internal force vector \mathbf{p} is given by

$$\mathbf{p} = A_0 s_{11} L \mathbf{B} \quad (14)$$

The stiffness matrix \mathbf{K} is obtained by the derivation of internal force vector \mathbf{p} to the node displacement vector \mathbf{d}

$$\mathbf{K} = \frac{\partial \mathbf{p}}{\partial \mathbf{d}} = A_0 L \mathbf{B} \frac{\partial s_{11}}{\partial \mathbf{d}} + A_0 L s_{11} \frac{\partial \mathbf{B}}{\partial \mathbf{d}} = \mathbf{K}_M + \mathbf{K}_G \quad (15)$$

Where, \mathbf{K}_M stands for material stiffness matrix, \mathbf{K}_G stands for geometric stiffness matrix. And

$$\frac{\partial s_{11}}{\partial \mathbf{d}} = \frac{\partial (s_0 + E e_{11})}{\partial \mathbf{d}} = E \frac{\partial e_{11}}{\partial \mathbf{d}} = E \mathbf{B} \quad (16)$$

Therefore

$$\begin{cases} \mathbf{K}_M = EA_0 L \mathbf{B}^T \mathbf{B} \\ \mathbf{K}_G = A_0 L s_{11} \frac{\partial \mathbf{B}}{\partial \mathbf{d}} \end{cases} \quad (17)$$

In which

$$\{\mathbf{K}_M\}_{3(i-1)+k, 3(a-1)+b} = \begin{cases} \frac{EA_0 l^2}{L^3} \left(-\frac{\Delta_k}{l_1} + \frac{\Delta_{3(n-1)+k}}{l_n} \right) \left(-\frac{\Delta_n}{l_1} + \frac{\Delta_{3(n-1)+b}}{l_n} \right) & i=1; k=1,2,3 \\ & a=1; b=1,2,3 \\ \frac{EA_0 l^2}{L^3} \left(-\frac{\Delta_k}{l_1} + \frac{\Delta_{3(n-1)+k}}{l_n} \right) \left(\frac{\Delta_{3(a-2)+b}}{l_{a-1}} - \frac{\Delta_{3(a-1)+b}}{l_a} \right) & i=1; k=1,2,3 \\ & a=2, \dots, n; b=1,2,3 \end{cases} \quad (18)$$

$$\{\mathbf{K}_M\}_{3(i-1)+k, 3(a-1)+b} = \begin{cases} \frac{EA_0 l^2}{L^3} \left(\frac{\Delta_{3(i-1)+k}}{l_{i-1}} - \frac{\Delta_{3(i-1)+k}}{l_i} \right) \left(-\frac{\Delta_n}{l_1} + \frac{\Delta_{3(n-1)+b}}{l_n} \right) & i=2, \dots, n; k=1,2,3 \\ & a=1; b=1,2,3 \\ \frac{EA_0 l^2}{L^3} \left(\frac{\Delta_{3(i-1)+k}}{l_{i-1}} - \frac{\Delta_{3(i-1)+k}}{l_i} \right) \left(\frac{\Delta_{3(a-2)+b}}{l_{a-1}} - \frac{\Delta_{3(a-1)+b}}{l_a} \right) & i=2, \dots, n; k=1,2,3 \\ & a=2, \dots, n; b=1,2,3 \end{cases} \quad (19)$$

$$\mathbf{K}_G = A_0 L s_{11} \frac{\partial \mathbf{B}}{\partial \mathbf{d}} = A_0 L s_{11} \frac{\partial \left(\frac{l}{L^2} \frac{\partial l}{\partial \mathbf{d}} \right)}{\partial \mathbf{d}} = \frac{A_0 s_{11}}{L^2} \left(\frac{\partial l}{\partial \mathbf{d}} \frac{\partial l}{\partial \mathbf{d}} + l \frac{\partial^2 l}{\partial \mathbf{d}^2} \right) \quad (20)$$

$$\left\{ \frac{\partial l}{\partial \mathbf{d}} \frac{\partial l}{\partial \mathbf{d}} \right\}_{3(i-1)+k, 3(a-1)+b} = \begin{cases} \left(-\frac{\Delta_k}{l_1} + \frac{\Delta_{3(n-1)+k}}{l_n} \right) \left(-\frac{\Delta_n}{l_1} + \frac{\Delta_{3(n-1)+b}}{l_n} \right) & i=1; k=1,2,3 \\ & a=1; b=1,2,3 \\ \left(-\frac{\Delta_k}{l_1} + \frac{\Delta_{3(n-1)+k}}{l_n} \right) \left(\frac{\Delta_{3(a-2)+b}}{l_{a-1}} - \frac{\Delta_{3(a-1)+b}}{l_a} \right) & i=1; k=1,2,3 \\ & a=2, \dots, n; b=1,2,3 \end{cases} \quad (21)$$

$$\left\{ \frac{\partial l}{\partial \mathbf{d}} \frac{\partial l}{\partial \mathbf{d}} \right\}_{3(i-1)+k, 3(a-1)+b} = \begin{cases} \frac{EA_0 l^2}{L^3} \left(\frac{\Delta_{3(i-1)+k}}{l_{i-1}} - \frac{\Delta_{3(i-1)+k}}{l_i} \right) \left(-\frac{\Delta_n}{l_1} + \frac{\Delta_{3(n-1)+b}}{l_n} \right) & i=2, \dots, n; k=1, 2, 3 \\ & a=1; b=1, 2, 3 \\ \frac{EA_0 l^2}{L^3} \left(\frac{\Delta_{3(i-1)+k}}{l_{i-1}} - \frac{\Delta_{3(i-1)+k}}{l_i} \right) \left(\frac{\Delta_{3(a-2)+b}}{l_{a-1}} - \frac{\Delta_{3(a-1)+b}}{l_a} \right) & i=2, \dots, n; k=1, 2, 3 \\ & a=2, \dots, n; b=1, 2, 3 \end{cases} \quad (22)$$

$$\left\{ \frac{\partial^2 l}{\partial \mathbf{d}^2} \right\}_{3(i-1)+k, 3(a-1)+b} = \begin{cases} \frac{1}{l_1} + \frac{1}{l_n} + \frac{\Delta_k^2}{l_1^3} + \frac{\Delta_{3(n-1)+k}^2}{l_n^3} & i=1; k=1, 2, 3 \\ \frac{1}{l_1} + \frac{1}{l_n} + \frac{\Delta_k^2}{l_1^3} + \frac{\Delta_{3(n-1)+k}^2}{l_n^3} & i=a; k=b \\ \frac{\Delta_k \Delta_b}{l_1^3} + \frac{\Delta_{3(n-1)+k} \Delta_{3(n-1)+b}}{l_n^3} & i=1; k=1, 2, 3 \\ \frac{\Delta_k \Delta_b}{l_1^3} + \frac{\Delta_{3(n-1)+k} \Delta_{3(n-1)+b}}{l_n^3} & i=a; k \neq b \end{cases} \quad (23)$$

$$\left\{ \frac{\partial^2 l}{\partial \mathbf{d}^2} \right\}_{3(i-1)+k, 3(a-1)+b} = \begin{cases} -\frac{1}{l_n} + \frac{\Delta_{3(n-1)+k}^2}{l_n^3} & i=1; k=1, 2, 3 \\ -\frac{1}{l_n} + \frac{\Delta_{3(n-1)+k}^2}{l_n^3} & a=n; k=b \\ \frac{\Delta_{3(n-1)+k} \Delta_{3(n-1)+b}}{l_n^3} & i=1; k=1, 2, 3 \\ \frac{\Delta_{3(n-1)+k} \Delta_{3(n-1)+b}}{l_n^3} & a=n; k \neq b \end{cases} \quad (24)$$

$$\left\{ \frac{\partial^2 l}{\partial \mathbf{d}^2} \right\}_{3(i-1)+k, 3(a-1)+b} = \begin{cases} -\frac{1}{l_1} + \frac{\Delta_k^2}{l_1^3} & i=1; k=1, 2, 3 \\ -\frac{1}{l_1} + \frac{\Delta_k^2}{l_1^3} & a=1; k=b \\ \frac{\Delta_k \Delta_b}{l_1^3} & i=1; k=1, 2, 3 \\ \frac{\Delta_k \Delta_b}{l_1^3} & a=1; k \neq b \end{cases} \quad (25)$$

$$\left\{ \frac{\partial^2 l}{\partial \mathbf{d}^2} \right\}_{3(i-1)+k, 3(a-1)+b} = \begin{cases} 0 & i=1; k=1, 2, 3 \\ 0 & a \neq 1, 2, n; k=1, 2, 3 \end{cases} \quad (26)$$

$$\left\{ \frac{\partial^2 l}{\partial \mathbf{d}^2} \right\}_{3(i-1)+k, 3(a-1)+b} = \begin{cases} \frac{1}{l_{i-1}} + \frac{1}{l_i} + \frac{\Delta_{3(i-2)+k}^2}{l_{i-1}^3} + \frac{\Delta_{3(i-1)+k}^2}{l_i^3} & i=2, \dots, n-1; k=1, 2, 3 \\ \frac{1}{l_{i-1}} + \frac{1}{l_i} + \frac{\Delta_{3(i-2)+k}^2}{l_{i-1}^3} + \frac{\Delta_{3(i-1)+k}^2}{l_i^3} & a=i; k=b \\ \frac{\Delta_{3(i-2)+k} \Delta_{3(a-2)+b}}{l_{i-1}^3} + \frac{\Delta_{3(i-1)+k} \Delta_{3(a-1)+b}}{l_i^3} & i=2, \dots, n-1; k=1, 2, 3 \\ \frac{\Delta_{3(i-2)+k} \Delta_{3(a-2)+b}}{l_{i-1}^3} + \frac{\Delta_{3(i-1)+k} \Delta_{3(a-1)+b}}{l_i^3} & a=i; k \neq b \end{cases} \quad (27)$$

$$\left\{ \frac{\partial^2 l}{\partial \mathbf{d}^2} \right\}_{3(i-1)+k, 3(a-1)+b} = \begin{cases} \frac{1}{l_{i-1}} + \frac{\Delta_{3(i-2)+k}^2}{l_{i-1}^3} & i=2, \dots, n-1; k=1, 2, 3 \\ \frac{1}{l_{i-1}} + \frac{\Delta_{3(i-2)+k}^2}{l_{i-1}^3} & a=i-1; k=b \\ \frac{\Delta_{3(i-2)+k} \Delta_{3(i-2)+b}}{l_{i-1}^3} & i=2, \dots, n-1; k=1, 2, 3 \\ \frac{\Delta_{3(i-2)+k} \Delta_{3(i-2)+b}}{l_{i-1}^3} & a=i-1; k \neq b \end{cases} \quad (28)$$

$$\left\{ \frac{\partial^2 l}{\partial \mathbf{d}^2} \right\}_{3(i-1)+k, 3(a-1)+b} = \begin{cases} \frac{1}{l_i} + \frac{\Delta_{3(i-1)+k}^2}{l_i^3} & i=2, \dots, n-1; k=1, 2, 3 \\ \frac{1}{l_i} + \frac{\Delta_{3(i-1)+k}^2}{l_i^3} & a=i+1; k=b \\ \frac{\Delta_{3(i-1)+k} \Delta_{3(i-1)+b}}{l_{i-1}^3} & i=2, \dots, n-1; k=1, 2, 3 \\ \frac{\Delta_{3(i-1)+k} \Delta_{3(i-1)+b}}{l_{i-1}^3} & a=i+1; k \neq b \end{cases} \quad (29)$$

$$\left\{ \frac{\partial^2 l}{\partial \mathbf{d}^2} \right\}_{3(i-1)+k, 3(a-1)+b} = 0 \quad \begin{array}{l} i = 2, \dots, n-1; k = 1, 2, 3 \\ a \neq i-1, i, i+1; k = 1, 2, 3 \end{array} \quad (30)$$

$$\left\{ \frac{\partial^2 l}{\partial \mathbf{d}^2} \right\}_{3(i-1)+k, 3(a-1)+b} = \begin{cases} \frac{1}{l_{n-1}} + \frac{1}{l_n} + \frac{\Delta_{3(n-2)+k}^2}{l_{n-1}^3} + \frac{\Delta_{3(n-1)+k}^2}{l_n^3} & i = n; k = 1, 2, 3 \\ \frac{1}{l_{n-1}} + \frac{1}{l_n} + \frac{\Delta_{3(n-2)+k}^2}{l_{n-1}^3} + \frac{\Delta_{3(n-1)+k}^2}{l_n^3} & i = a; k = b \\ \frac{\Delta_{3(n-2)+k} \Delta_{3(n-2)+b}}{l_n^3} + \frac{\Delta_{3(n-1)+k} \Delta_{3(n-1)+b}}{l_n^3} & i = n; k = 1, 2, 3 \\ \frac{\Delta_{3(n-2)+k} \Delta_{3(n-2)+b}}{l_{n-1}^3} + \frac{\Delta_{3(n-1)+k} \Delta_{3(n-1)+b}}{l_n^3} & i = a; k \neq b \end{cases} \quad (31)$$

$$\left\{ \frac{\partial^2 l}{\partial \mathbf{d}^2} \right\}_{3(i-1)+k, 3(a-1)+b} = \begin{cases} -\frac{1}{l_{n-1}} - \frac{\Delta_{3(n-2)+k}^2}{l_{n-1}^3} & i = n; k = 1, 2, 3 \\ -\frac{1}{l_{n-1}} - \frac{\Delta_{3(n-2)+k}^2}{l_{n-1}^3} & a = n-1; k = b \\ \frac{\Delta_{3(n-2)+k} \Delta_{3(n-2)+b}}{l_{n-1}^3} & i = n; k = 1, 2, 3 \\ \frac{\Delta_{3(n-2)+k} \Delta_{3(n-2)+b}}{l_{n-1}^3} & a = n-1; k \neq b \end{cases} \quad (32)$$

$$\left\{ \frac{\partial^2 l}{\partial \mathbf{d}^2} \right\}_{3(i-1)+k, 3(a-1)+b} = \begin{cases} -\frac{1}{l_n} - \frac{\Delta_{3(n-1)+k}^2}{l_n^3} & i = n; k = 1, 2, 3 \\ -\frac{1}{l_n} - \frac{\Delta_{3(n-1)+k}^2}{l_n^3} & a = 1; k = b \\ \frac{\Delta_{3(n-1)+k} \Delta_{3(n-1)+b}}{l_n^3} & i = n; k = 1, 2, 3 \\ \frac{\Delta_{3(n-1)+k} \Delta_{3(n-1)+b}}{l_n^3} & a = 1; k \neq b \end{cases} \quad (33)$$

$$\left\{ \frac{\partial^2 l}{\partial \mathbf{d}^2} \right\}_{3(i-1)+k, 3(a-1)+b} = 0 \quad \begin{array}{l} i = n; k = 1, 2, 3 \\ a \neq n-1, n, 1; k = 1, 2, 3 \end{array} \quad (34)$$

It is noted that when the arbitrary adjacent two nodes along the cable coincide with each other, the length between these two nodes is zero and the stiffness matrix is singular. In this case the analytical method must be adopted. But, as far as the structural problems are concerned, the amount of node sliding is usually small relative to the cable segment length. It seldom occurs that the stiffness matrix is singular in the structural analysis. When two adjacent nodes do not coincide with each other, the length between adjacent nodes will never be zero.

2.2 Element mass and force

In a total Lagrange formulation, the element mass matrix and body force vector are typically formulated only once on the initial configuration. For the closed sliding polygonal cable element, however, the element mass matrix and body force vector must be updated by a nonlinear iteration.

For a two-node cable element, its element mass matrix is given by

$$M_2 = \int_{V_0} \rho \mathbf{N}^T \mathbf{N} dV_0 = \frac{\rho A_0 l L}{6} \frac{1}{l} \begin{bmatrix} 2\mathbf{I} & \mathbf{I} \\ \mathbf{I} & 2\mathbf{I} \end{bmatrix}_{6 \times 6} = \frac{\rho A_0 L}{6} \begin{bmatrix} 2\mathbf{I} & \mathbf{I} \\ \mathbf{I} & 2\mathbf{I} \end{bmatrix}_{6 \times 6} \quad (35)$$

where \mathbf{N} is the element shape function, \mathbf{I} is a 3×3 identity matrix, ρ is the density (assuming it is constant). A_0 is the initial cross-sectional area (assuming it is constant), l is the current element length, and L is the initial element length.

For the n-node closed sliding polygonal cable element, the cable joints divide it into n straight segments, each with two nodes. Therefore, the mass matrix of the n-node closed sliding polygonal cable element in the current configuration is obtained simply by assembling the individual mass matrices for each part using Eq. (35) and the current lengths. Therefore, the mass matrix for then-node closed sliding polygonal cable element is given by

$$\mathbf{M} = \sum_{i=1}^{N-1} \frac{\rho A_0 L l_i}{2l} \begin{bmatrix} 0 & 0 & 0 & 0 & 0 \\ 0 & \mathbf{I} & 0 & 0 & 0 \\ 0 & 0 & \mathbf{I} & 0 & 0 \\ 0 & 0 & 0 & \cdot & 0 \\ 0 & 0 & 0 & 0 & 0 \end{bmatrix}_{3N \times 3N} \quad (36)$$

The element body force, due to self-weight, is formulated in a similar manner. For an two-node cable element

$$\mathbf{F}_T = \int_{V_0} \mathbf{N}^T f^B dV_0 = \frac{\rho A_0 L}{2} \begin{Bmatrix} \mathbf{g} \\ \mathbf{g} \end{Bmatrix}_{6 \times 1} \quad (37)$$

where $f^B = \rho g$ is the weight per unit volume, and g is the gravity vector given by

$$\mathbf{g} = \{g_x \ g_y \ g_z\}^T \quad (38)$$

The body force for an n-node closed sliding polygonal cable element, therefore

$$F = \sum_{i=1}^{N-1} \frac{\rho A L l_i}{2l} \begin{bmatrix} 0 \\ \cdot \\ \mathbf{g} \\ \mathbf{g} \\ 0 \end{bmatrix}_{3N \times 1} \quad (39)$$

2.3 Realization of the closed sliding polygonal cable element

According to the above deduction and the function of self-defined element subroutine UEL in finite element analytical software ABAQUS, the program for sliding polygonal element with arbitrary number nodes is implemented using the program language of FORTRAN, and the program is used as a structural element of ABAQUS to simulate and analyze structural problems containing sliding polygonal cable elements. The self-defined element subroutine of the sliding polygonal cable element with nodes of arbitrary number is utilized to investigate the following three cases.

3. Verification

This example was used to verify the validity of internal force vector and the stiffness matrix of the closed sliding polygonal cable element. Fig. 2 shows that the four-segment length of a four-

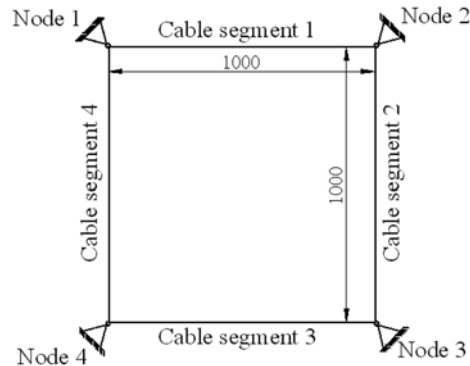


Fig. 2 Four-node closed sliding polygonal cable element

node closed sliding polygonal cable element are 1000 mm; The diameter and Yong's modulus of the cables are assumed to be 30 mm and 20000 kN/mm², respectively; and its linear thermal expansion coefficient is 1.87×10^{-5} . All bearings are fixed, but the nodes attached to the bearings allow the cable sliding. A minus temperature difference of 80°C was applied on the cable Segment 1. The stiffness of cable element is assumed to be infinite. The total length of cable element will keep constant in the whole sliding process. The weight of the four-node closed sliding polygonal cable element was ignored. So the analytical solution of internal force in each cable segment is 54.5 kN.

This problem was solved by the developed program of the closed sliding polygonal cable element in ABAQUS, and the internal force of each cable segment was obtained. The force was 54.8 kN with an error of 0.5%. Therefore, the solution with the finite element analysis of the sliding polygonal cable element was quite precise for engineering, which validated that the internal force vector and stiffness matrix of closed sliding polygonal cable element were accurate enough.

4. Application 1: structural analysis of suspen-dome structures with sliding cable joints

4.1 The studied suspen-dome structure

In order to study the structural behavior of suspen-dome structures with sliding cable joints, a suspen-dome structure was designed. This suspen-dome structure was with a span of 91.4 m and a rise of 17.03 m. Steel pipes of $\phi 203 \text{ mm} \times 6 \text{ mm}$, $\phi 219 \text{ mm} \times 7 \text{ mm}$, $\phi 245 \text{ mm} \times 7 \text{ mm}$, $\phi 273 \text{ mm} \times 8 \text{ mm}$, $\phi 299 \text{ mm} \times 8 \text{ mm}$ were used as the principal members of the upper single layer shell, and steel pipes of $\phi 219 \text{ mm} \times 7 \text{ mm}$ were used as vertical struts. Seven radial steel bars ($\phi 80 \text{ mm}$) and seven hoop cables ($\phi 7 \text{ mm} \times 121$) were arranged in the bottom of the structure. The elastic modulus of steel and cable were $2.1 \times 10^5 \text{ N/mm}^2$ and $1.8 \times 10^5 \text{ N/mm}^2$, respectively. The boundary conditions were assumed to be simply supported. The pre-stresses of hoop cables were uniformly set as 127 kN, 420 kN, 390 kN, 530 kN, 810 kN, 1242 kN, 2060 kN. The finite element model is shown in Fig. 3 and Fig. 4.

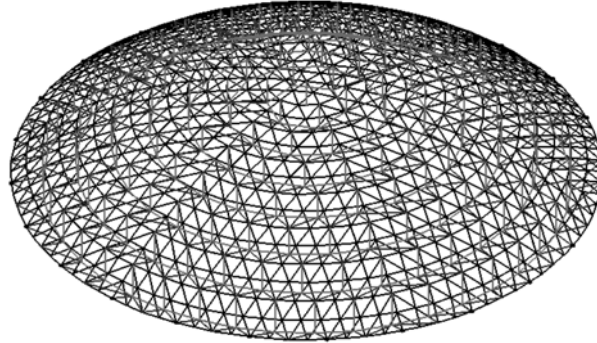


Fig. 3 Axonometric view of suspen-dome structure

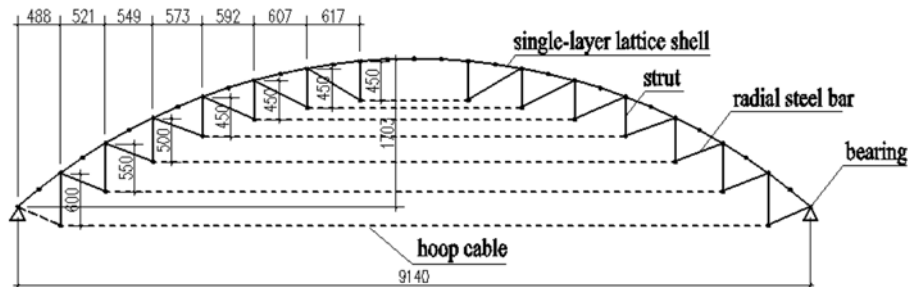


Fig. 4 Sectional view of suspen-dome structure

5.2 Structural behavior of suspen-dome with sliding cable joints

Two finite element models were established with the commercial finite element software ABAQUS, as shown in Fig. 3. The closed sliding polygonal cable element presented in this paper was implemented in ABAQUS as a user defined element and seven elements were adopted for the seven rings of latitudinal cables of Model-A. For the sake of comparison, the latitudinal cables of Model-B were assumed to be separated by adjacent joints, and 2-node linear displacement 3-D truss element, T3D2, was adopted for the cable segments. The element selection for other members was all same for Model-A and Model-B, as shown in Table 1. The material property of steel cables was set to be of no compression.

In order to consider the effect of the rise-span ratios on the structural behavior of suspen-dome structures, one model was designed with rise-span ratios of 0.1 for Model-A and Model-B, respectively. On the other hand, in order to consider the effect of the type of boundary conditions on the structural behavior of suspen-dome structures, one model was designed that only DZ degrees of freedom degree was restricted for Model-A and Model-B, respectively. As previously stated, there were totally six models designed for this study as listed in Table 2.

According to the conclusions of Reference (Chen 2010), the sliding of the latitudinal cables has little effect on static behaviour and nonlinear stability of the suspen-dome under symmetric loads. Therefore, only asymmetric loads were considered in this paper.

The cable force for three models with sliding cable joints and three models without sliding cable

Table 1 Element type for finite element models

Members	Element type	
	Model-A	Model-B
Single-layer lattice dome	B33 (2-node 3-D cubic beam element)	
Strut	T3D2 (2-node linear displacement 3-D truss element)	
Radial cables	T3D2 (No compression)	
Latitudinal cables	Closed sliding polygonal cable element	T3D2 (No compression)

Table 2 Model description

Model Num	Rise-to-span	Bearing type	Cable joint type
Model-A -1	0.25	DX, DY, DZ	Sliding
Model-A -2	0.1	DX, DY, DZ	Sliding
Model-A -3	0.25	DZ	Sliding
Model-B -1	0.25	DX, DY, DZ	No sliding
Model-B -2	0.1	DX, DY, DZ	No sliding
Model-B -3	0.25	DZ	No sliding

Table 3 Cable force in suspen-dome under asymmetric loads

Cable number	1	2	3	4	5	6	7
Model-B-1 F-Max	8.3	45.4	86.4	192.5	177.0	297.7	516.9
Model-B-1 F-Min	31.3	74.6	115.8	220.6	196.4	316.5	590.7
Model-B-1 deviation	277.7	64.3	34.1	14.6	11.0	6.3	14.3
Model-A -1 Cable force	19.2	58.7	98.6	203.7	183.5	290.6	448.0
Model-B-2 F-Max	0.0	26.0	70.4	180.6	184.2	316.9	472.7
Model-B-2 F-Min	38.3	99.4	162.6	269.5	245.9	387.2	636.7
Model-B-2 deviation		282.8	131.1	49.2	33.5	22.2	34.7
Model-A -2 Cable force	18.2	63.1	115.5	216.3	200.8	315.2	466.0
Model-B-3 F-Max	6.6	44.9	84.8	189.5	171.2	170.0	329.9
Model-B-3 F-Min	32.5	75.4	115.9	219.8	195.3	305.0	486.3
Model-B-3 deviation	395.4	68.0	36.6	16.0	14.1	79.4	47.4
Model-A -3 Cable force	17.68	58.49	98.27	203.06	181.96	281.73	400.01

joints are listed in Table 3. It can be seen that the deviation for models without sliding cable joint is up to 395.4%, which revealed that the cable force for each hoop cable was highly non-uniform distributed under asymmetric loads. But if the sliding cable joint was adopted in suspen-dome structures, the distribution of the cable force for each hoop cable was uniform. Furthermore, compared with the models without sliding cable joints, the cable force of the model with sliding cable joints is very smaller than that of the counterpart, which is helpful for improving the material

Table 4 The maximum nodal displacement, maximum member stress of upper single dome and the stability bearing capacity

Model number	U-MAX	S-MAX	P_{cr}
Model-B-1	0.03	87.07	29.30
Model-A -1	0.07	204.90	21.60
$100 \times (\text{Model-A -1} - \text{Model-B-1}) \div \text{Model-B-1}$	95.03	135.33	-26.28
Model-B-2	0.09	96.19	14.62
Model-A -2	0.14	139.60	6.49
$100 \times (\text{Model-A -2} - \text{Model-B-2}) \div \text{Model-B-2}$	55.15	45.13	-55.61
Model-B-3	0.07	209.90	27.93
Model-A -3	0.07	234.40	16.56
$100 \times (\text{Model-A -3} - \text{Model-B-3}) \div \text{Model-B-3}$	5.90	11.67	-40.71

utilization efficiency of the cables.

The maximum nodal displacement, maximum member stress of the upper single dome and the stability bearing capacity for three models with sliding cable joints and three models without sliding cable joint are listed in Table 4. Compared with three models without sliding cable joints, the U-MAX and S-MAX was increased by up to 95.03% and 135.33%, respectively. Compared with three models without sliding cable joints, the P_{cr} was reduced by a decrease of 55.61%. Therefore, the structural behavior of suspen-dome without sliding cable joints is better than that of the suspend-domes with sliding cable joints.

5. Application 2: structural analysis of cable dome structures with sliding cable joint

5.1 The studied cable dome structure

In order to study the structural behavior of cable dome structures with sliding cable joints, a cable dome was designed as shown in Fig. 5. The span of this cable dome is 120 m. The area and prestressing of all members are described in the Fig. 6 and Table 5. The nodal load for each node is 600kN in the following analysis. The Young's modulus of cable and struts are $E = 185 \times 10^6$ kN/m² and $E = 210 \times 10^6$ kN/m², respectively.

Two finite element models were established with the commercial finite element software ABAQUS. The closed sliding polygonal cable element presented in this paper was implemented in ABAQUS as a user defined element and two elements were established for the two rings of latitudinal cables of Model-A. For the sake of comparison, the latitudinal cables of Model-B were assumed to be separated by adjacent joints and 2-node linear displacement 3-D truss element, T3D2, was adopted for the cable segments. The element selection for other members is all same for Model-A and Model-B and they were simulated by 2-node linear displacement 3-D truss element, T3D2. The material property for steel cables was set to be of no compression.

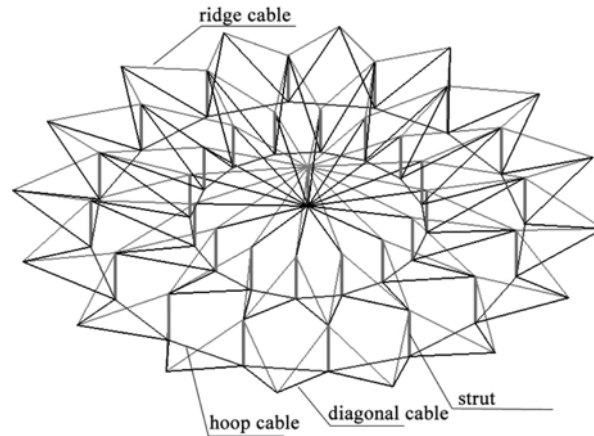


Fig. 5 Axonometric view of cable dome structure

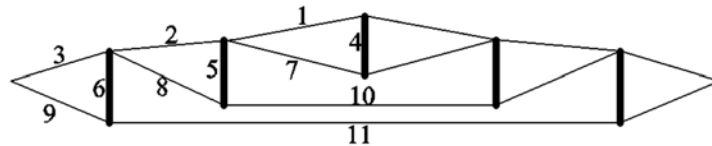


Fig. 6 Member number referred by Table 5

Table 5 the area and pre-stressing for all members

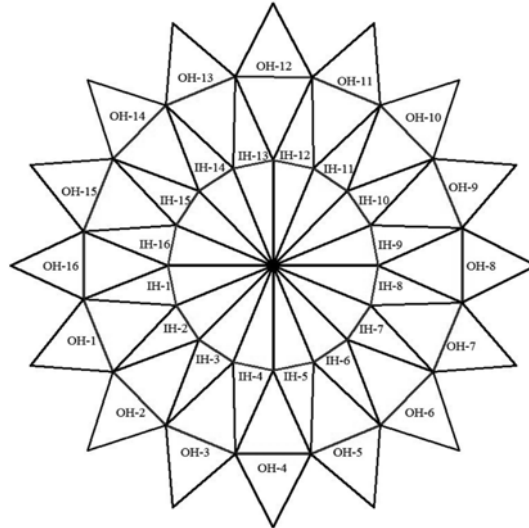
Element Num	1	2	3	4	5	6
Area (cm ²)	16.2	16.2	16.2	158.3	27.5	99.0
Pre-stressing (kN)	760	688	1075	-2000	-130	-550
Element Num	7	8	9	10	11	
Area (cm ²)	10.9	10.9	32.5	32.5	129.9	
Pre-stressing (kN)	515	165	791	712	2988	

5.2 Structural behaviors of the cable dome structures considering the cable sliding

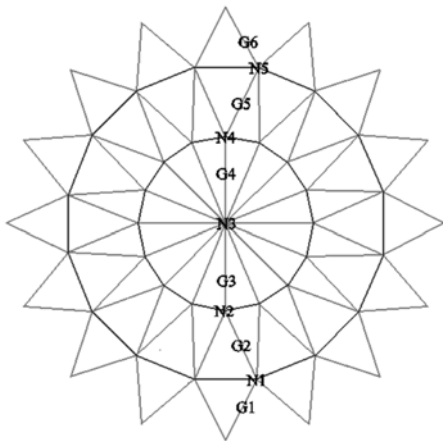
The members of cable dome structures were pre-tensioned before applying the loads to produce initial stiffness. The pre-stressing forces listed in Table 5 were applied as initial stresses. Two loading cases were considered in this study, one is about symmetric loads, and the other about is asymmetric loads. The static analysis results were carried out for two above load cases.

The inner hoop cable number and the outer hoop cable number referred by the analysis are shown in Fig. 7. The node number (from N1 to N5) and ridge cable number (from G1 to G5) referred by the analysis are shown in Fig. 8. The strut number (from S1 to S5) and diagonal cable number (from D1 to D5) referred by the analysis are shown in Fig. 9.

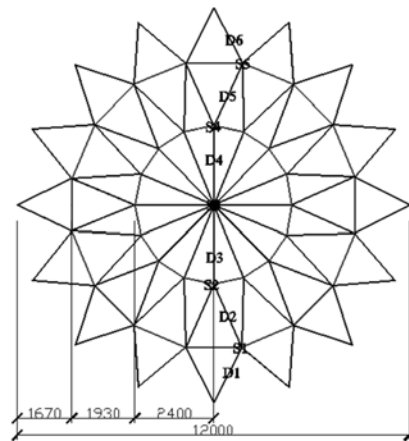
The static analysis results of both Model-A and Model-B is shown in Figs. 10-15. Compared with Model-B, the member stress and nodal displacement of Model-A was similar to that of Model-B under all-span load. Therefore, the sliding of the latitudinal cables had little effect on the static



IH- denotes the inner hoop cables; OH- denotes the outer hoop cables
 Fig. 7 Hoop cable number referred by result analysis in Fig. 10 and Fig. 11



N- denotes the node numbers referred by Fig. 12
 G- denotes the ridge cable numbers referred by Fig. 13
 Fig. 8 Node number and ridge cable number referred by result analysis



S- denotes the strut numbers referred by Fig. 14
 D- denotes the diagonal cable numbers referred by Fig. 15
 Fig. 9 Strut number and diagonal cable number referred by result analysis

behaviour of the cable domes under symmetric loads (all span loads).

It can be seen from Fig. 10 and Fig. 11 that the stress of hoop cables was no-uniform for Model-B but the stress is uniform for Model-A under half span load. Compared with Model-B, the maximum axial stress of the inner hoop cable and outer hoop cable in Model-A was reduced by 26.48% 37.99%, respectively, which is helpful for improving the material utilization efficiency of the cables.

It can be seen from Fig. 12 to Fig. 15 that the maximum nodal displacement, maximum stress of

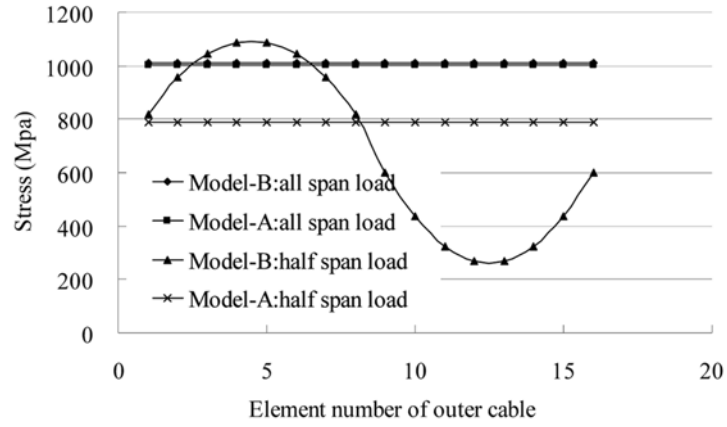


Fig. 10 Axial stress of outer hoop cables of Model-A and Model-B

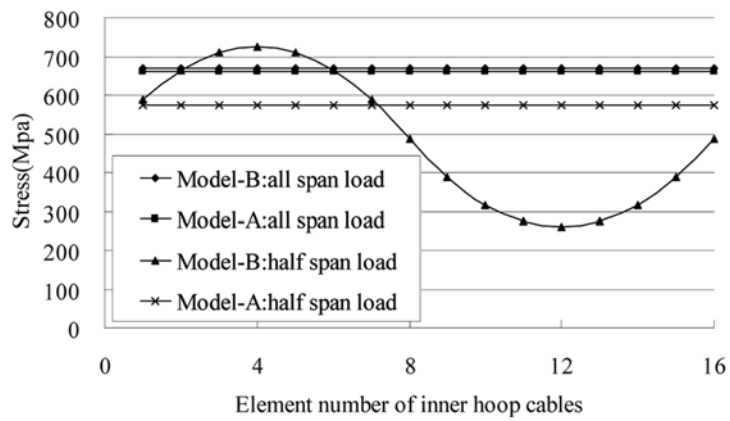


Fig. 11 Axial stress of inner hoop cables of Model-A and Model-B

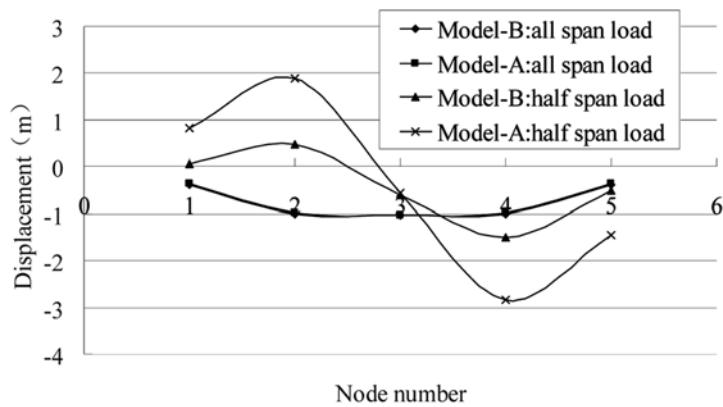


Fig. 12 Nodal displacement of Model-A and Model-B

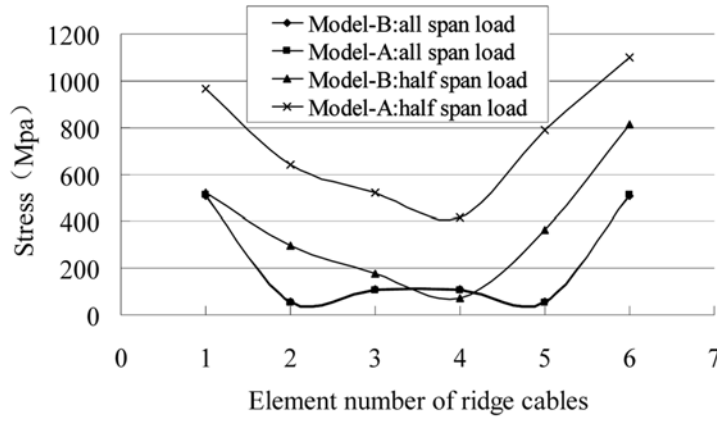


Fig. 13 Axial stress of ridge cables of Model-A and Model-B

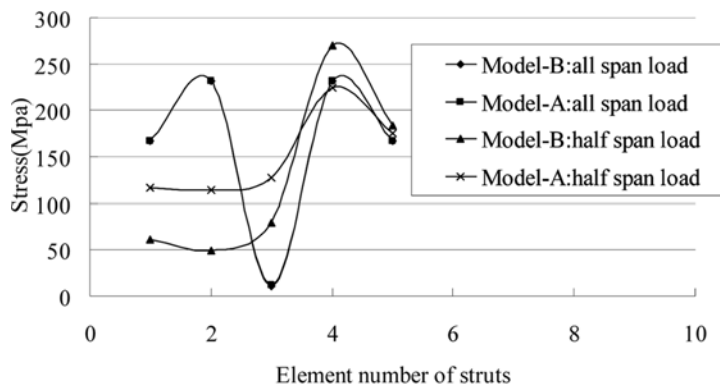


Fig. 14 Axial stress of struts of Model-A and Model-B

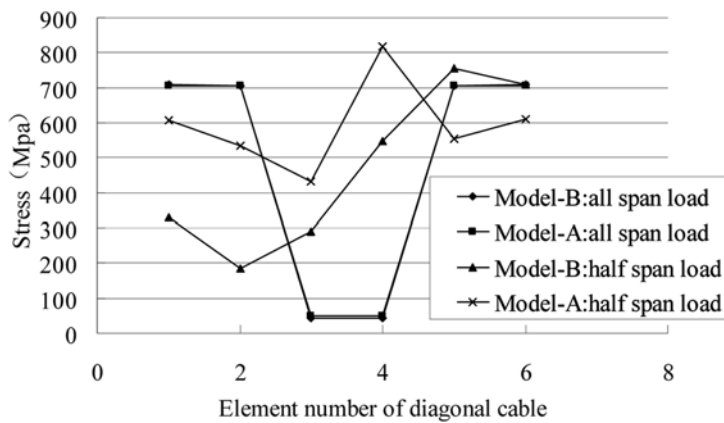


Fig. 15 Axial stress of diagonal cables of Model-A and Model-B

strut, maximum stress of ridge cable and diagonal cable of Model-A were increased by 88.8%, -17.8%, 35.4% and 8.5%, respectively, compared to that of Model-B. Therefore, the sliding the latitudinal cables had a significant effect on the static behaviour and nonlinear stability of the suspen-dome under asymmetric loads (half span loads).

6. Conclusions

In order to study the structural behavior of the cable dome structures and the suspen-dome structures with sliding cable joints, the tangent stiffness matrix of a closed sliding polygonal cable element was derived. Then the closed sliding polygonal cable element was implemented in the commercial finite element software ABAQUS as a user defined element and applied in the static analysis of a suspen-dome structure and a cable dome structure. The following conclusions were made:

- 1) The rationality and effectiveness of the presented closed sliding polygonal cable element was verified for the simulation of sliding situations.
- 2) With the sliding cable joints, uniform axial force distribution can be achieved for the hoop cables of the suspen-dome and cable dome, which is helpful for improving the material utilization efficiency of the cables and preventing the cables from slacking under asymmetric loads.
- 3) If the measure of no sliding cable joint is adopted, the adjacent members will share some displacement and member stress. If local nodal displacement or member stress is extreme large, therefore, the structural behavior of suspen-dome and cable dome without sliding cable joints is better than that with sliding cable joints.

Acknowledgements

This work is sponsored by the National Natural Science Foundation of China and China Postdoctoral Science Foundation funded project.

References

- Cao, Q.S. and Zhang, Z.H. (2010), "A simplified strategy for force finding analysis of suspendomes", *Eng. Struct.*, **32**(1), 306-310.
- Chen, Z.H., Wu, Y.J., Yin, Y. and Shan, C. (2010), "Formulation and application of multi-node sliding cable element for the analysis of Suspen-Dome structures", *Finite Elem. Anal. Des.*, **46**(9), 743-750.
- Chen, Z.H., Liu, H.B., Wang, X.D. and Zhou, T. (2011), "Establishing and application of cable-sliding criterion equation", *Adv. Steel Constr.*, **7**(2), 131-143.
- Chen, Z.H. and Wu, Y.J. (2010), "Design of roll cable-strut joint in suspen-dome and analysis of its application in whole structure system", *J. Build. Struct.*, **31**(1), 234-240.
- Chen, Z.H. and Li, Y. (2005), "Parameter analysis on stability of a suspen-dome", *Int. J. Space Struct.*, **20**(2), 115-124.
- Cui, X.Q. and Guo, Y.L. (2004), "Influence of gliding cable joint on mechanical behavior of suspen-dome structures", *Int. J. Space Struct.*, **19**(3), 149-154.
- Geiger, D.H., Stefaniuk, A. and Chen, D. (1986), "The design and construction of two cable domes for the Korean Olympics", *Proceedings of the IASS Symposium on Shells, Membranes and Space Frames*, Vol. 2,

- Osaka, Japan.
- Kang, W.J., Chen, Z.H., Lam, H.F., and Zuo, C.R. (2003), "Analysis and design of the general and outmost-ring stiffed suspen-dome structures", *Eng. Struct.*, **25**(13), 1685-1695.
- Kitipornchai, S., Kang, W.J., Lam, H.F. and Albermani, F. (2005), "Factors affecting the design and construction of lamella suspen-dome systems", *J. Constr. Steel Res.*, **61**(6), 764-785.
- Kawaguchi, M., Tatemichi, I. and Chen, P.S. (1999), "Optimum shapes of a cable dome structure", *Eng. Struct.*, **21**(8), 719-725.
- Kawaguchi, M., Abe, M. and Tatemichi, I. (1999), "Design, tests and realization of 'suspen-dome' System", *J IASS*, **40**(131), 179-192.
- Kim, S.D., Kim, H.S. and Kang, M.M. (2003), "A study of the nonlinear dynamic instability of hybrid cable dome structures", *Struct. Eng. Mech.*, **15**(6), 653-668.
- Wang, S., Zhang, G.J., Zhang, A.L., Ge, J. and Qin, J. (2007), "The prestress loss analysis of cable-strut joint of the badminton gymnasium for 2008 Olympic Games", *J. Build Struct.*, **28**(6), 39-44.
- Yuan, X.F. and Dong, S.L. (2002), "Nonlinear analysis and optimum design of cable domes", *Eng. Struct.*, **24**(7), 965-977.
- Yuan, X.F., Chen, L.M. and Dong, S.L. (2007), "Prestress design of cable domes with new forms", *Int. J. Solids Struct.*, **44**(9), 2773-2782.
- Yuan, X.F. and Dong, S.L. (2003), "Integral feasible prestress of cable domes", *Comput. Struct.*, **81**(21), 2111-2119.
- Zhang, A.L., Liu, X.C., Wang, D.M., Wei, W.H., Huang, D.M., Wu, L.Y. and Li, Z.G. (2007), "Static experimental study on the model of the suspend-dome of the badminton gymnasium for 2008 Olympic Games", *J. Build Struct.*, **28**(6), 58-67.
- Zhang, Z.H., Cao, Q.S., Dong, S.L. and Fu, X.Y. (2008), "Structural design of a practical suspendome", *Adv. Steel Constr.*, **4**(4), 323-340.
- Zhou, B., Accorsi, M.L. and Leonard, J.W. (2004), "Finite element formulation for modeling sliding cable elements", *Comput. Struct.*, **82**(2-3), 271-280.